been studied in some detail. Although they exhibit g values characteristic of sodium metal, it is clear that these spectra are not consistent with a simple metal particles model, and that talk of quantum size effects in such systems is premature.

Initially when sodium atoms enter Na-Y, they are ionized, and the valence electrons thus released are trapped in the sodalite cages to form Na_4^{3+} centers. It is the cornerstone of our interpretation that centers located in adjacent sodalite cages are sufficiently close to one another that they are coupled strongly through the exchange interaction, resulting in the loss of hyperfine structure and a featureless singlet ESR line. The concept of domains of interacting paramagnetic centers enables many other features associated with the ESR of the inclusion compounds of sodium in zeolites X, Y, and A to be rationalized. The fall in line width of the ESR singlet in Na/Na-Y with increasing concentration of included metal may be ascribed to increasing domain size, and the eventual slow increase in line width which accompanied decomposition of the zeolite framework at high concentrations of metal may be accounted for by a return to smaller domains as the structure collapsed. The characteristic line shape, with more intensity in the wings than a Lorentzian line, can also be explained by the presence of a distribution of line widths due to different domain sizes. Lastly, the model is consistent with the important observation that the intensity of the singlet line increases at low temperature.

The emphasis of the basic model on the interaction between stable paramagnetic centers located in the sodalite cage limits its validity to relatively low concentrations of included metal, before the sodalite cages become saturated. In contrast, the ESR spectra are observed to evolve gradually as the zeolites accommodate sodium far in excess of this amount. Evidence from both ESR and ^{23}Na NMR suggests that, whatever their precise location, the surplus valence electrons are also able to interact with their neighbors and contribute to the singlet ESR line. The continued decrease in line width with increasing sodium concentration may thus be attributed to a decrease in the average distance between interacting electrons, as Na_4^{3+} becomes one of many possible paramagnetic centers all interacting together in a "paramagnetic soup". At high concentrations of included sodium there is some evidence of mobility, of either atoms, ions, or electrons, and a motional contribution to line-narrowing. A reason for the unusual nature of the variation of the singlet line width with temperature in the three zeolites considered may therefore be found in the conflicting effects of an increase in T_2 and a reduction in the narrowing frequency.

In the absence of framework degradation, the characteristic g values of the compounds we have studied are fully consistent with those recorded previously for sodium metal or metal particles (Table I). The fact that *liquid* sodium[31] exhibits the same g value is proof aplenty that the observation of this value is not indicative of the presence of the bulk lattice or, indeed, of any particular structure. The results presented here indicate that it may well be contingent only on the fact of interaction between sodium valence electrons. At any rate, it is abundantly clear that extreme caution must be exercised in the assignment of unexplained ESR lines to particulate or "colloidal" sodium.

In this paper we have developed a description of the inclusion compounds of sodium in zeolites which is consistent with a wide range of detailed experimental observations. Casting the incoming sodium atoms in the role of electron donors, and focusing on the interaction of the released electrons both with the sodium ions of the zeolite framework and with each other, it provides an entirely new conceptual framework for the study of this class of compounds and indicates that they will make an important contribution to our understanding of the metal-nonmetal transition.

Acknowledgment. We thank the Department of Education for Northern Ireland, B.P. (VRU), and the SERC for financial support. The ESR simulation program was written by Dr. R. J. Singer.

Structural Information of the Nitrogenase Metal Clusters Deduced from Paramagnetic Interactions

Melinda E. Oliver and Brian J. Hales*

Contribution from the Department of Chemistry, Louisiana State University, Baton Rouge, Louisiana 70803. *Received April 27, 1992*

Abstract: The MoFe-protein (component 1) of nitrogenase contains two major classes of metal clusters, called P and M. In the as-isolated form of the protein, the P-clusters are diamagnetic while the M-centers are paramagnetic, yielding an EPR spectrum of an $S = {}^3/_2$ species. This protein was titrated with thionin to oxidize the P-clusters, converting them into paramagnetic species while preserving the paramagnetism of the M-centers. During this titration, the relaxation properties of the protein's M-centers were monitored with an EPR spectrometer using the technique of progressive power saturation. The results obtained using this technique demonstrate the existence of a perturbation of the relaxation times (T_1T_2) of the M-centers induced by the presence of the paramagnetic P-clusters. The magnetic interaction that induces this perturbation depends on the orientation of the MoFe-protein in the spectrometer's magnetic field and, therefore, is probably dipolar in origin. Furthermore, the nonlinear relationship between the magnitude of this perturbation and the extent of oxidation of the P-clusters can be interpreted in terms of a semi-interactive model in which four P-clusters are grouped as two interactive pairs. In this model, the magnitude of the magnetic interaction between the P-cluster pairs and the M-centers is greater when one P-cluster is oxidized than when both clusters of the same interactive pair are oxidized. This model further shows that, while the P-clusters of the resting enzyme are diamagnetic, the 1- and 2-equiv oxidized forms of the P-cluster pairs can both be paramagnetic.

Nitrogenase catalyzes the biological reduction of dinitrogen to ammonia. The conventional form of the enzyme consists of two distinct proteins, both necessary for enzymatic activity. One of the proteins (called component 1 or the MoFe-protein) contains 30-33 Fe and 2 Mo atoms in various metal clusters and possesses the sites for substrate reduction.

Characterization of component 1 by EPR, Mössbauer, X-ray absorption, ESEEM,[1] MCD, and ENDOR spectroscopies has

0002-7863/92/1514-10618$03.00/0

greatly enhanced our understanding of the metal clusters present in this protein. In general, there are two major classes of metal clusters, labeled M and P from Mössbauer studies.[2,3] The M-centers (two per component 1 protein) have a composition[4,5] of 1:6–8:8–10 Mo:Fe:S in an unknown structure. These centers (also termed FeMoco for FeMo-cofactor) can be extracted from active protein and used to reconstitute activity in cofactor-less component 1 and are believed to be at or near the site of substrate reduction. In the as-isolated form of the protein in the presence of dithionite, the M-centers are paramagnetic[2] with a spin state of $S = {}^3/_2$ and effective g-factors of 4.3, 3.6, and 2.0 but convert to a diamagnetic state upon oxidation of the protein.

The P-clusters of the MoFe-protein can be extracted as [4Fe–4S] clusters by core extrusion.[6] However, Mössbauer[7] and MCD[8] spectroscopic studies suggest them to be a novel form of cluster with electronic transitions different from those observed for conventional [4Fe–4S] clusters. On the basis of these extraction studies as well as Mössbauer quantitation data, it generally has been believed that there are four P clusters per MoFe-protein,[3] although recently two eight-Fe-containing clusters have been proposed.[9-11] Regardless of their structure, MCD studies show that P-clusters are conserved in nitrogenases isolated from diverse nitrogen-fixing organisms including the alternative vanadium form of the enzyme.[12]

In the as-isolated form of the protein, the P-clusters are diamagnetic but become paramagnetic when oxidized. Mössbauer studies[3] suggest an $S = {}^3/_2 - {}^9/_2$ state for this paramagnetism while magnetization curves from MCD studies[8] have indicated a probable $S = {}^5/_2 - {}^7/_2$ spin state. Recently, EPR spectra[10] of component 1 oxidized in the presence of solid thionin exhibit a signal associated with an $S = {}^7/_2$ state, tentatively assigned to oxidized P-clusters.

Obviously, one of the major questions in the research involving nitrogenase has been the structure/function relationship of the different metal clusters. This paper represents the first in a series which investigates the structures of the various metal clusters in the nitrogenase enzyme proteins by using progressive power saturation techniques with an EPR spectrometer. Specifically, other than recent preliminary X-ray diffraction data,[13] little is known about either the structural arrangement of the P-clusters in component 1 or their possible interactions with the M-centers. In this publication, progressive power saturation technique is used to probe the extent of magnetic interactions between P-clusters and M-centers during oxidative titrations. The results of this study show the presence of such interactions and are interpreted in terms of a semi-interactive model in which the four P-clusters are not independent but are grouped as two interactive pairs. This data also shows the existence of different magnetic properties for the 1- and 2-equiv oxidized forms of these interactive pairs of P-clusters.

Materials and Methods

Sample Preparation. Component 1 from *Azotobacter vinelandii* (Av1) was isolated and purified using published procedures.[14] Acetylene reduction was used as a monitor of activity as previously described.[15] Av1 with specific activities in the range 1100–1500 nmol C_2H_2 reduced min^{-1} mg^{-1} protein was used.

Thionin-oxidized samples were prepared in the following manner. Av1 was reduced with dithionite (2 mM) in the presence of methyl viologen (5 μM), to ensure complete reduction of all the different metal clusters, and subsequently eluted on an G-25 column (0.5 × 10 cm) in an anaerobic chamber to rid the protein of excess dithionite, methyl viologen, and residual salt. A solution of thionin, which had been prepared anaerobically and its concentration determined optically at 602 nm (ϵ_{602} = 56 300 cm^{-1} M^{-1}), was titrated into the protein sample until a faint blue hue persisted for about 5 min. The final concentration of thionin was assumed to be that required for oxidation of 6 equiv, and correspondingly, one-sixth of this concentration was assumed as the amount necessary for 1 equiv (i.e., oxidation of one of the six clusters of component 1).

Progressive Power Saturation. For each set of experiments, seven EPR tubes, each containing Av1 and enough thionin (as determined above) for 0–6 equiv of oxidized sample, were prepared. Progressive power saturation studies were performed on these samples as outlined in the results section. Because of the short Av1 relaxation times at temperatures above 8 K, spectra were recorded at the lowest possible temperature (typically 3.8 K). This low temperature was necessary in order to observe significant power saturation of the Av1 signal and, therefore, allow us to be able to detect the small differences in power saturation data that occurred in our experiments. Due to the strong temperature-dependency of the saturation parameters of a paramagnetic center at these low temperatures, great care was taken to control the temperature to ±0.1 K. As an added precaution to eliminate progressive errors, power settings for a given temperature were randomly chosen and all data sets for each comparative study were performed on the same day. It has been shown[16] that strong dipole–dipole interactions can affect the saturation profile of a paramagnet. However, due to the orientation selectivity of our experiment, this phenomenon is less important to our work. Finally, spectra were tested at modulation frequencies lower than 100 kHz, typically used for EPR detection, to ensure the absence of significant saturation transfer at these low temperatures.

Saturation data were obtained for the M centers of Av1 during different stages of thionin oxidation on four separate trials. These data were normalized and averaged to further reduce small random fluctuations in different data sets. It is important to note, however, that the same trend in saturation data was always observed for all the different data sets.

EPR spectra were recorded on a Bruker ER300D spectrometer interfaced to a Bruker 1600 computer for data storage and manipulation. Low temperatures were achieved using an Oxford Instrument ESR-9 flow cryostat (3.8 to 300 K) positioned in a TE_{102} cavity, resonating at X-band frequencies. Temperatures were monitored using an Oxford Instruments Model ITC4 temperature controller with a digital readout.

Results and Discussion

Both chemical[3,17,18] and electrochemical[19] oxidations of nitrogenase component 1 have been studied extensively in order to gain a better understanding of electron flow between the P-clusters and M-centers in this protein. Most of these oxidations occur in two phases which have been interpreted as follows: initially the diamagnetic ($S = 0$) P-clusters are oxidized to a paramagnetic ($S = {}^3/_2 - {}^9/_2$) state followed by the oxidation of the paramagnetic ($S = {}^3/_2$) M-centers to a diamagnetic state with a subsequent loss

(1) Abbreviations: Av1, MoFe-protein of conventional nitrogenase from *Azotobacter vinelandii*; ESEEM, electron spin echo envelope modulation; ENDOR, electron nuclear double resonance; MCD, magnetic circular dichroism.

(2) Münck, E.; Rhodes, H.; Orme-Johnson, W. H.; Davis, L. C.; Brill, W. J.; Shah, V. K. *Biochim. Biophys. Acta* **1975**, *400*, 32–53.

(3) Zimmerman, R.; Münck, E.; Brill, W. J.; Shah, V. K.; Henzl, M. T.; Rawlings, J.; Orme-Johnson, W. H. *Biochim. Biophys. Acta* **1978**, *537*, 185–207.

(4) Yang, S. S.; Pan, M. A.; Friesen, G. D.; Burgess, B. K.; Corbin, J. L.; Stiefel, E. I.; Newton, W. E. *J. Biol. Chem.* **1982**, *257*, 8042–8048.

(5) Nelson, M. J.; Levy, M. A.; Orme-Johnson, W. H. *Proc. Natl. Acad. Sci. U.S.A.* **1983**, *80*, 147–150.

(6) Kurtz, D. M.; McMillan, R. S.; Burgess, B. K.; Mortenson, L. E.; Holm, R. H. *Proc. Natl. Acad. Sci. U.S.A.* **1979**, *76*, 4986.

(7) Huynh, B. H.; Henzl, M. T.; Chritner, J. A.; Zimmermann, R.; Orme-Johnson, W. H.; Münck, E. *Biochim. Biophys. Acta* **1980**, *623*, 124–138.

(8) Johnson, M. K.; Thomson, A. J.; Robinson, A. E.; Smith, B. E. *Biochim. Biophys. Acta* **1981**, *671*, 61–70.

(9) Orme-Johnson, W. H.; Lindahl, P.; Meade, J.; Warren, W.; Nelson, M.; Groh, S.; Orme-Johnson, N. R.; Münck, E.; Huynh, B. H.; Emptage, M.; Rawlings, J.; Smith, J.; Roberts, J.; Hoffmann, B.; Mims, W. B. In *Current Perspectives in Nitrogen Fixation*; Gibson, A. H., Newton, W. E., Eds.; Elsevier: North-Holland, New York, 1981; pp 79–84.

(10) Hagen, W. R.; Wassink, H.; Eady, R. R.; Smith, B. E.; Haaker, H. *Eur. J. Biochem.* **1987**, *169*, 457–465.

(11) Müller, A.; Knüttel, E.; Hildebrand, A.; Bögge, H.; Schneider, K.; Armatage, A. *Naturwissenschaften* **1991**, *78*, 460–462.

(12) Morningstar, J. E.; Johnson, M. K.; Case, E. E.; Hales, B. J. *Biochemistry* **1987**, *26*, 1795–1800.

(13) Bolin, J. T.; Ronco, A. E.; Mortenson, L. E.; Morgan, T. V.; Williamson, M.; Xuong, N.-H. In *Nitrogen Fixation: Achievements and Objectives*; Gresshoff, P. M., Roth, L. E., Stacey, G., Newton, W. E., Eds.; Chapman and Hall: New York, 1990; pp 117–124.

(14) Burgess, B. K.; Jacobs, D. B.; Steifel, E. I. *Biochim. Biophys. Acta* **1980**, *614*, 196–209.

(15) Hales, B. J.; Langosch, D. J.; Case, E. E. *J. Biol. Chem.* **1986**, *261*, 15301–15306.

(16) Hirsh, D. J.; Beck, W. F.; Innes, J. B.; Brudvig, G. W. *Biochemistry* **1992**, *31*, 532–541.

(17) Watt, G. D.; Burns, A.; Lough, S.; Tennent, D. L. *Biochemistry* **1980**, *19*, 4926–4932.

(18) Watt, G. D.; Burns, A.; Tennent, D. L. *Biochemistry*, **1981**, *20*, 7272–7277.

(19) Watt, G. D. *Anal. Biochem.* **1979**, *99*, 399–407.

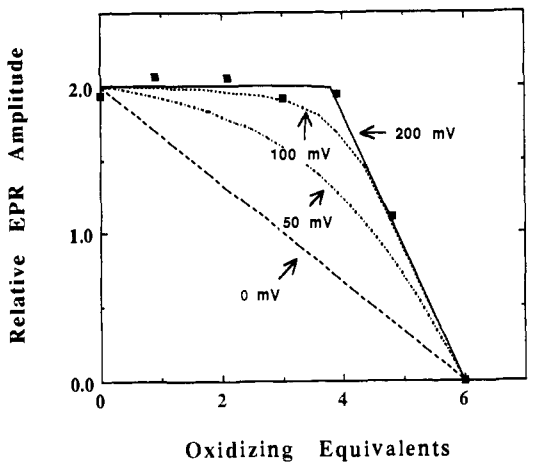

Figure 1. Relative EPR amplitude of the $g = 3.64$ inflection for the $S = {}^3/_2$ signal of the M-center in Avl plotted (■) as a function of the number of equivalents of thionin per protein added to solution. Titration is based on the assumption that Avl requires 6 equiv for complete oxidation. Also shown are theoretical plots of one-electron oxidative titrations of six independent redox centers; four of the centers (P) have identical redox midpoints of E_0' while the remaining two (M) centers have redox midpoints of $E_0' + \Delta E$. For these plots, only the extent of reduction of the M-centers is being monitored during the oxidation. Listed next to each plot is the value of ΔE. Note that when $\Delta E = 0$, all six centers have the same midpoint and a linear change in the relative amount of reduced M is observed during the oxidation, while for $\Delta E \geq 200$ mV, the plot is similar to the experimental data.

of the characteristic $S = {}^3/_2$ EPR spectrum. For example,[3,17] when thionin is used as the oxidizing agent of Avl, it takes 3–4 equiv to oxidize the P-clusters with an additional 2–3 equiv to oxidize the M-centers.

We have repeated this titration using thionin with similar results. Specifically, upon addition of each oxidizing equivalent to component 1, the EPR spectrum of the M-centers was monitored by measuring the amplitude of the $g = 3.6$ inflection of the $S = {}^3/_2$ EPR signal. In agreement with previous results,[3] the amplitude of this signal remained approximately constant up to about 4 oxidizing equiv added (Figure 1), suggesting little if any oxidation of the M-centers during these initial steps. However, upon addition of the 5th equiv, the amplitude of the $g = 3.6$ EPR signal fell to about half the previous amplitude while the 6th equiv almost completely quenched the EPR spectrum, again implying that the 5th and 6th equiv oxidize the M-centers, rendering them EPR silent.

In the interpretation of the data in Figure 1, it has been assumed that, during thionin oxidation of Avl, the P-clusters are all oxidized before the M-centers. This interpretation implies that the oxidation midpoint potential of the P-clusters is very different from that of the M-centers. To test the validity of this assumption, relative amplitudes of the M-centers' EPR signals were calculated during oxidative titration of component 1. In these calculations, coupled Nernst equations were used with the condition that the four P-clusters are each 1-equiv oxidized with the same redox midpoint potential of E_0' while the two M-centers have midpoint potentials of $E_0' + \Delta E$. If the P-clusters and the M-centers have the same midpoints (i.e., $\Delta E = 0$ mV), the amplitude of the M-centers' EPR signals will decrease linearly with oxidizing equivalents (Figure 1). In this situation the theoretical curve mimics the data obtained for component 1 from *Clostridium pasteurianum* when oxidized by either indigodisulfonate or methylene blue.[20] On the other hand, the $\Delta E = 100$ mV curve is similar to the data obtained by Watt et. al[18] for either thionin or methylene blue oxidation of Avl. Since our data best fits the curve for large ΔE (≥200 mV), the assumption that only P-clusters are oxidized during the first 4 equiv is reasonable. This conclusion is also in agreement with results obtained from potentiometric reductive titrations[17] which suggest $\Delta E = 190$ mV.

As mentioned above, both Mössbauer[3] and MCD[8,12] spectroscopic studies of component 1 have demonstrated that the P-clusters become paramagnetic upon oxidation with thionin. However, in spite of their paramagnetism, to date no EPR spectrum has been reported to be associated with them, an unusual result, if one assumes that the paramagnetism of the fully oxidized P-clusters is associated with a Krammer's state. The data shown in Figure 1 suggest an interesting situation. Namely, during the initial four oxidation steps, the P-clusters become paramagnetic while the M-centers remain paramagnetic. If this is true, examination of the relaxation properties of the EPR spectrum of the M-centers during this titration should indicate whether these centers are close enough to the P-clusters to experience magnetic interactions from them.

To investigate this, the relaxation properties of the M-centers were monitored during the thionin titration. Portis[21] and Castner[22] first evaluated the relationship between power saturation and relaxation times of paramagnetic resonances. For such samples, the amplitude, A, of the derivative EPR spectrum is related to the incident microwave power, P, by the expression

$$A = K\sqrt{P}\Big/(1 + P/P_{1/2})^{b/2} \qquad (1)$$

where K is a proportionality factor and $P_{1/2}$ is the microwave power needed for half-saturation of the signal and is proportional to $1/g^2T_1T_2$. In this latter term, g is the magnetogyric ratio of the paramagnetic, T_1 is its spin–lattice relaxation time, and T_2 its spin–spin relaxation time. The exponent b in eq 1 is referred to as the inhomogeneity factor. For inhomogeneously broadened lines, such as those observed for most metalloproteins, $b = 1$.

Beinert and Orme-Johnson[23] showed that eq 1 can be rearranged to

$$A/\sqrt{P} = K(P_{1/2})^{b/2}/(P_{1/2} + P)^{b/2}$$

and, taking the logarithm, yields

$$\log (A/\sqrt{P}) = -b/2 \log (P_{1/2} + P) + b/2 \log (P_{1/2}) + \log (K) \quad (2)$$

The value of $P_{1/2}$ can be determined from progressive saturation experiments by plotting eq 2 as $\log (A/\sqrt{P})$ vs $\log P$. In such a plot, two linear regions are observed, one at low power (i.e., no observed saturation or $P \ll P_{1/2}$) and the second at high power (i.e., pronounced saturation or $P \gg P_{1/2}$). The value of the power at which the straight lines representing these two linear regions intersect is $P_{1/2}$.

Obviously any perturbation, such as magnetic interaction between the P-clusters and M-centers, that influences either T_1 or T_2 will be reflected as a change in $P_{1/2}$. Therefore, using the progressive power saturation technique, $P_{1/2}$ values were determined for the M-centers of Avl during different stages of thionin oxidation. Figure 2 exhibits a plot of eq 2 for the amplitude of the $g = 3.64$ inflection of the M-center's EPR spectrum of Avl both in the as-isolated state (0e) and after the addition of 1 equiv of thionin (1e). In the work presented here, the values of $P_{1/2}$ were determined by fitting eq 2 to the experimental data. The increase in $P_{1/2}$ upon addition of the first oxidizing equivalent suggests that the P-clusters and M-centers are close enough to each other for magnetic interactions to occur between them.

In Figure 3, $\Delta P_{1/2}$, the increase in $P_{1/2}$ relative to the as-isolated protein, is plotted for each oxidizing equivalent. This plot shows that, contrary to what might be expected to happen as more P-clusters become paramagnetic, the additions of the 2nd and 3rd equiv do not continue to cause a significant increase in $\Delta P_{1/2}$. In fact, $\Delta P_{1/2}$ remains approximately constant and even decreases with the fourth addition, at which point, presumably, all of the P clusters are oxidized and paramagnetic.

(20) Morgan, T. V.; Mortenson, L. E.; McDonald, J. W.; Watt, G. D. *J. Inorg. Chem.* **1988**, *33*, 111–120.

(21) Portis, A. M. *Phys. Rev.* **1956**, *104*, 584–588.

(22) Castner, T. G., Jr. *Phys. Rev.* **1959**, *115*, 1506–1515.

(23) Beinert, H.; Orme-Johnson, W. H. In *Magnetic Resonance in Biological Systems*; Ehrenberg, A., Malström, B. G., Vänngard, T., Eds.; Pergamon Press: Oxford, England, 1967; pp 221–247.

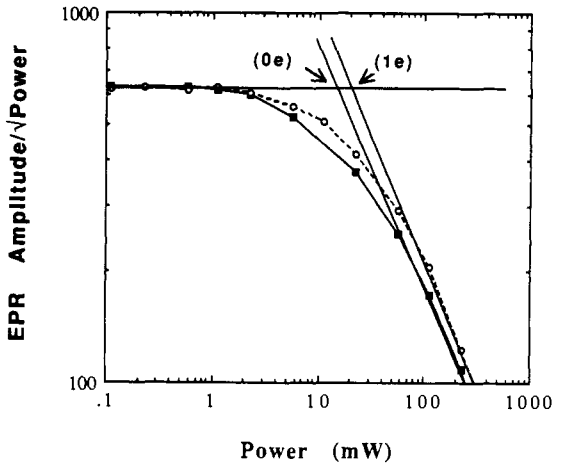

Figure 2. Example of data obtained from progressive power saturation experiment on EPR spectrum of Av1. In this example only part of the actual 10-nW–600-mW data is shown for clarity. Amplitude of $g = 3.64$ inflection of the M-center of Av1 was monitored as a function of the incident microwave power and plotted according to eq 2 in the text. Data was collected for the protein in the as-isolated state (Oe; ■), where all of the P-clusters are reduced and diamagnetic, as well as the 1-equiv oxidized state (1e; O), where, on the average, one P-cluster per protein is oxidized. Power settings were randomly chosen and temperature was maintained at 3.8 ± 0.1 K. In this figure the arrows point to the different values of $P_{1/2}$ as determined for the two different systems. The value of $P_{1/2}$ was determined by fitting the experimental data to eq 2 in the text.

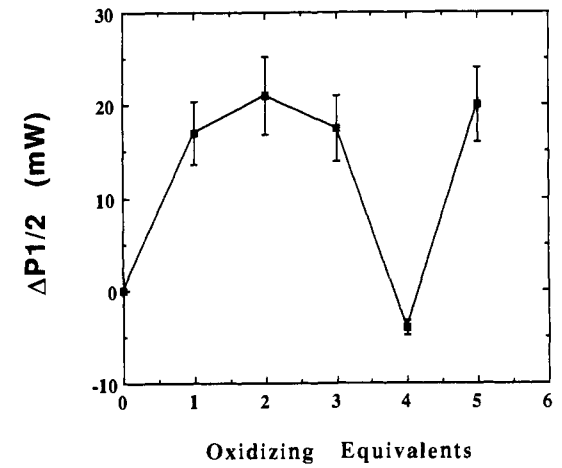

Figure 3. Plot of increase in $P_{1/2}$ (i.e., $\Delta P_{1/2}$ where $P_{1/2}$ for the as-isolated protein is the reference point) for M-centers of Av1 as monitored at the $g = 3.64$ inflection during oxidative titration with thionin at 3.8 K. Data represent the average $\Delta P_{1/2}$ of four separate experiments. Uncertainty calculated for data is represented as error bars.

In order to understand the meaning of this trend in the $\Delta P_{1/2}$ values with oxidation, several models of the arrangement of the P-clusters relative to the M-centers will be proposed. It has been suggested[24] that the two M-centers are separate, non-interacting entities. This suggestion recently has been strengthened by preliminary X-ray diffraction data[13] that imply that the M-centers are positioned at opposite ends of the component 1 protein. Because of this, in all of our models, the M-centers will be assumed to be independent entities. Therefore, the difference among each of these models which produces the observed variation in $\Delta P_{1/2}$ must be associated with differences in the arrangement of the P-clusters.

As mentioned above, there are two current hypotheses for the number and structure of the P-clusters in each protein. One theory[2] is that there are four distinct clusters with a possible

(24) Orme-Johnson, W. H.; Hamilton, W. D.; Ljones, T.; Tso, M.-Y.; Burris, R. H.; Shah, V. K.; Brill, W. J. *Proc. Natl. Acad. Sci. U.S.A.* **1972**, *69*, 3142–3145.

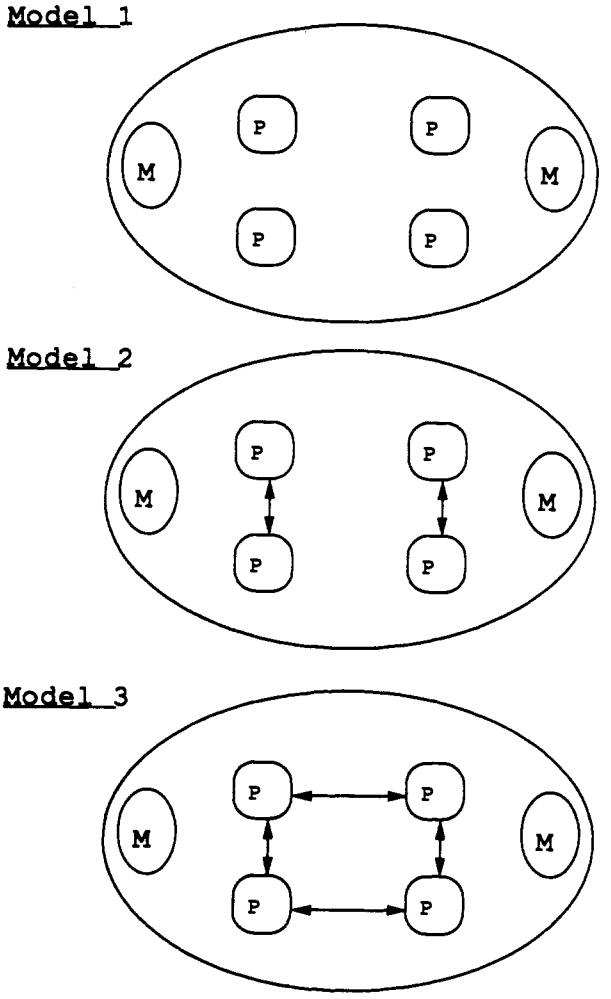

Figure 4. Three different models for the interactions among P-clusters (P) and M-centers (M) within a MoFe-protein. In these models, the double-headed arrows represent interacting P-clusters. In Model 1, all P-clusters are independent and non-interacting. In Model 2, the P-clusters are grouped as two interactive pairs while in Model 3 all four P-clusters interact with each other.

[4Fe–4S]-type of structure, while the second theory[9–11] predicts two large clusters with an eight-Fe nuclearity. Preliminary X-ray diffraction data[13] only detect four and not six major clusters and, therefore, favor the two-large-cluster model. However, for simplicity of our discussion, we will initially interpret our data in terms of four clusters.

Certain assumptions have been made in all of our models. (1) All the P-clusters have the same redox midpoint potential for oxidation. (2) The P-to-M interactions are all equivalent so that the oxidation of any one P-cluster produces the same magnetic interaction with the neighboring M-center. (3) Where appropriate, the P-clusters have been grouped in pairs, where each pair interacts with only one M-center. This final assumption is made for simplicity of the model; it will be shown later that these models predict the same variation in $\Delta P_{1/2}$ even when all four P-clusters are simultaneously, but differently, interacting with both M-centers.

In our first model (Figure 4), all four P-clusters are independent (i.e., $4 \times P$). This means that the magnitude of the effect that any one oxidized P-cluster has on the relaxation behavior of the neighboring M-center is independent of the oxidation states of the other P-clusters in the protein. As will be shown, in this model $\Delta P_{1/2}$ is approximately proportional to the number of paramagnetic P-clusters.

The second model groups the P-clusters in interactive pairs (i.e., $2 \times$ P–P). In this model, when both P-clusters in a given pair are oxidized (P^{Ox}–P^{Ox}), the magnetic perturbation experienced by the M-center is not doubled, as in the first model, but in fact is negated. In this model, an M-center experiences magnetic

perturbation only when one of the P-clusters in a pair is oxidized (P^{Ox}–P), not both. Antiferromagnetic coupling is an extreme example of this type of interaction.

Finally, in the third model, all four P-clusters are interactive (i.e., P_4). When any two of the clusters are oxidized (P_2^{Ox}–P_2), all magnetic interaction with the M-centers is quenched. Obviously, this last model, unlike the first two, implies that all of the P-clusters interact simultaneously with both M-centers.

Following oxidation by 1 equiv, magnetic interactions occur between P-clusters and M-centers for all three models, in agreement with the increase in $\Delta P_{1/2}$ following the 1st oxidizing equiv (Figure 4). Oxidation by the 2nd equiv, however, produces different effects in each model. In Model 1, because the P-clusters are non-interactive, the average magnetic effect experienced by the M-centers is just twice that of the first oxidation step. Conversely, in Model 3, because all of the P-clusters are interactive, an oxidation of any two of them causes a cancellation of the magnetic effect experienced by the M-centers.

Because the P-clusters are paired with each M-center in Model 2, however, double oxidation can occur by one of two modes which will be assumed to be of equal probability. In the first mode, one P-cluster from each pair is oxidized (i.e., P^{Ox}–P and P^{Ox}–P) so that the total magnetic interaction is twice that experienced for the first oxidation step. In the second mode, both P-clusters in one of the pairs are oxidized (i.e., P^{Ox}–P^{Ox} and P–P). Since oxidation has occurred in a pair of interactive P-clusters, the resultant magnetic effect is cancelled.

The overall effect, as monitored by $\Delta P_{1/2}$ with EPR spectroscopy, is double that of the 1st equiv for Model 1 and a negation for Model 3. However for Model 2, where half the M-centers experience a magnetic effect (i.e., mode one) and the other half experience no effect (mode two), the average interaction is identical to that following the 1st oxidizing equiv. In other words, Model 2 will show no change in $\Delta P_{1/2}$ between the first and second oxidation steps.

Continuing with this argument yields the theoretical $\Delta P_{1/2}$ predicted for each model during the first four oxidation steps. These results are shown in Figure 5, where it is obvious that the data in Figure 3 are best mimicked by Model 2.

Before discussing the significance of these results, it is helpful at this point to reconsider our initial assumptions, their validity, and how changing these assumptions might affect the results shown in Figure 5. One of the assumptions made was that, when oxidized, all of the P-clusters impose the same magnetic effect on the M-centers. However, because we have been assuming a statistical distribution of oxidize P-clusters, it can be easily seen that, even if the clusters were not equivalent, an average of all of the different magnetic effects is always observed. This is tantamount to each P-cluster imposing an effect equal to the average. Therefore, the results shown in Figure 5 do not change when the P-clusters are nonequivalent.

Another assumption that was not stated but was used in calculating the predictions shown in Figure 5 was that, following oxidation by m equiv ($m < 4$), *all* of the proteins had exactly m P-clusters oxidized; i.e., the 1st equiv oxidized *all* the proteins by 1 equiv, and so forth. However, because it was assumed that all of the P-clusters are identical (i.e., that they all have the same redox midpoint potential for oxidation), it is more probable that a statistical distribution of oxidations occurs among them. In other words, during each oxidation step, a statistical fraction of proteins will have no P-clusters oxidized, while others will have all of their clusters oxidized and the remainig proteins will contain a mixture of both oxidized and reduced P-clusters. Using a statistical weighting factor to take into consideration the results of a mixture of proteins at different stages of oxidation, new theoretical curves were calculated for each model and are also shown as dashed lines in Figure 5 where it is evident that both Model 2 and Model 3 mimic the experimental data. This result demonstrates that the *minimum* requirement needed to simulate the experimental data is the existence of an interaction between pairs of P-clusters (Model 2). Higher order interactions (Model 3) can also exist, but their presence does not dramatically influence the results. Unfortunately, our data cannot distinguish between the P-clusters being groups as four four-Fe clusters or two eight-Fe clusters. However, the interpretation of the data *does* require that the oxidations to the states P^{Ox}–P and P^{Ox}-P^{Ox} must be accomplished 1 equiv at a time (i.e., two one-electron oxidation steps as opposed to one two-electron step) where each oxidation has approximately the same midpoint potential.

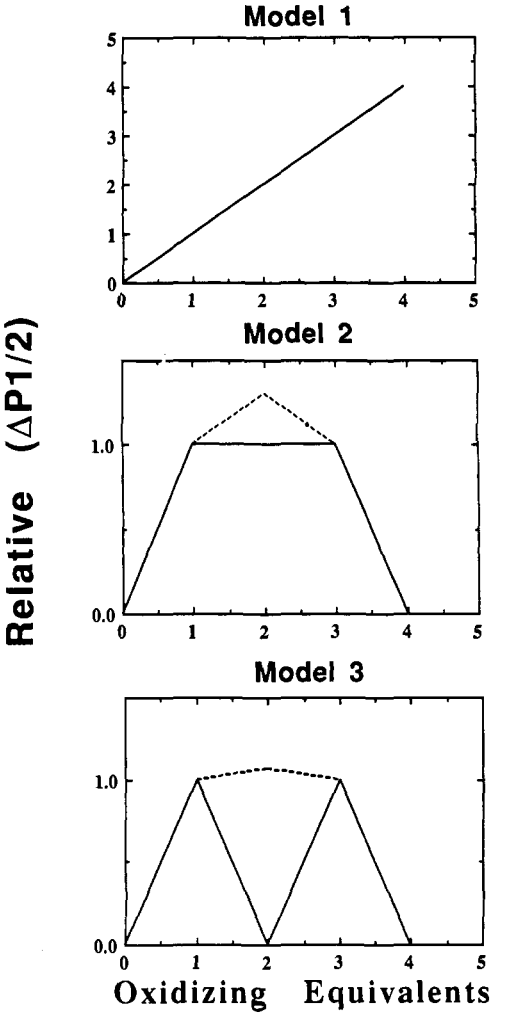

Figure 5. Theoretical prediction of variation in $\Delta P_{1/2}$ with oxidizing equivalents for the three different model systems shown in Figure 4. Solid lines represent predictions based on highly non-cooperative model initially proposed in the text. Dashed lines depict trends predicted when statistical averaging is introduced into calculations.

What is the origin of the magnetic interaction between the P-clusters and the M-centers? Equation 1 suggests that there is an induced change in the quantity $(1/T_1T_2)$ for the M-centers during the oxidation of the P-clusters. In general, magnetic interactions between different metal clusters have been found to be predominantly dipolar. Dipolar interactions will decrease T_1 and may also shorten the phase memory time, T_2, although this latter effect may not be significant in our situation, since measurable line broadening of the M-center's EPR signal was not observed during the oxidative titration. The dipolar contribution to $1/T_1$ (as well as $1/T_2$), and therefore $\Delta P_{1/2}$, can be expressed as a sum of interactive terms (i) which originate from the dipolar Hamiltonian and can generally be expressed[25-27] as

$$1/T_1 = J_P(J_P + 1)/r^6 \sum G_i(\Theta)F_i(T_{1P}) \qquad (3)$$

In this equation, J_P is the total angular momentum of the perturbing metal cluster (i.e, the 1-equiv oxidized P-cluster in our

(25) Bloembergen, N. *Physica* **1949**, *15*, 386–426.
(26) Abragam, A. *Phys. Rev.* **1955**, *98*, 1729–1735.
(27) Hyde, J. S.; Rao, K. V. S. *J. Magn. Reson.* **1978**, *29*, 509–516.

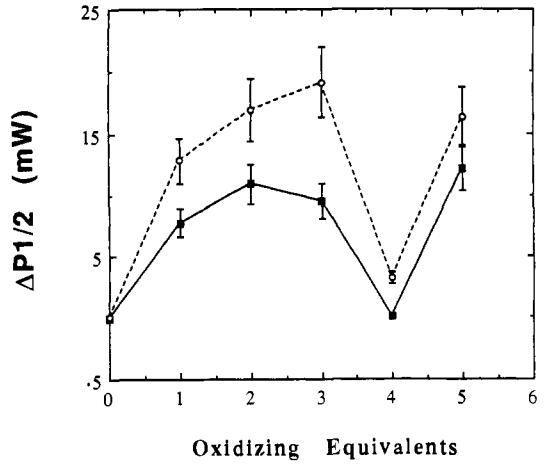

Figure 6. Variation of $\Delta P_{1/2}$ for the $S = {}^3/_2$ signal of M-centers of Av1 monitored simultaneously at both $g = 3.6$ (■) and $g = 4.3$ (○) inflections during oxidative titration with thionin at 4.1 K. Data represents the average change of four separate experiments. Error bars denote the expected uncertainty in each measurement.

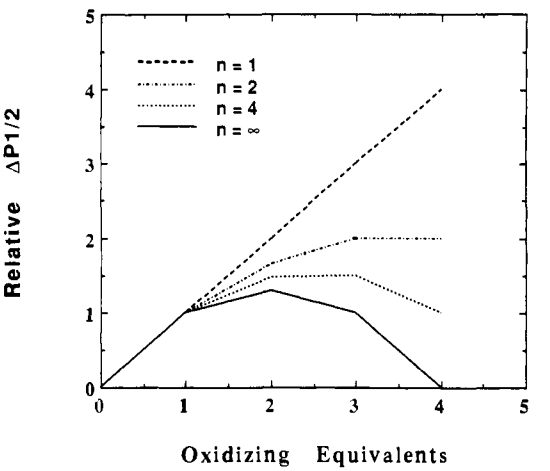

Figure 7. Theoretical prediction of the variation of $\Delta P_{1/2}$ with oxidizing equivalents. In this plot it is assumed that the product of oxidation of one of the P-clusters of an interactive pair (i.e., P^{Ox}–P) exhibits a magnetic interaction with the neighboring M-center to produce a $\Delta P_{1/2}$ of the amount α. When both P-clusters are oxidized (i.e., P^{Ox}–P^{Ox}), the M-center experienced a total interaction of $2\alpha/n$. When $n = 1$, the system behaves as predicted by Model 1, where the P-clusters are noninteractive, while $n = \infty$ assumes interacting P-clusters as described in Model 2 (see Figure 5). For $1 < n < \infty$, the P-clusters can be described as interactive yet with both P^{Ox}–P and P^{Ox}–P^{Ox} paramagnetic but with different spin properties.

experiment), $G_i(\Theta)$ is a function that depends on the angle Θ between the vector connecting the M-center to the paramagnetic P-cluster and the vector representing the direction of the EPR spectrometer's external magnetic field, r is the distance from the M-center to the P-cluster, and $F_i(T_{1P})$ is a function that depends on the spin–lattice relaxation time (T_{1P}) of the paramagnetic P-cluster. Using extrinsic paramagnetic probes, this equation previously has been used[27] to predict the magnitude of r for several metalloproteins. However, since we do not know J_P, Θ, or T_{1P} for the P-clusters, this distance cannot be calculated from our data.

Equation 3 suggests, if our interpretation of the data in Figure 3 is correct, any change in J_P, Θ, or T_{1P} may quantitatively (but *not* qualitatively) affect the variation of $\Delta P_{1/2}$ with oxidizing equivalents. For example, rotating the external magnetic field relative to the direction of the M-to-P vector will change Θ. The data in Figure 3 was obtained by positioning the magnetic field at the $g = 3.6$ resonance of Av1. This resonance is predominantly influenced by those Av1 molecules oriented with the y-axis of one of their M-centers parallel to the external magnetic field. By positioning the magnetic field at the $g = 4.3$ resonance, we would be selecting a new subset of Av1 molecules, namely those whose M-centers' x-axes are parallel to the external field. In other words, by positioning the magnetic field at different spectral inflections, we effectively select different values of Θ in eq 3 and should observe corresponding changes in $\Delta P_{1/2}$. To test the validity of using eq 3 in interpreting our data, $\Delta P_{1/2}$ values were again determined, this time simultaneously for both the $g = 3.6$ and $g = 4.3$ resonances. As predicted by eq 3, the magnitude of $\Delta P_{1/2}$ determined at the $g = 4.3$ resonance is significantly different from that determined at $g = 3.6$ (Figure 6) while the general variation in $\Delta P_{1/2}$ is similar, further strengthening our interpretation of the dipolar origin of $\Delta P_{1/2}$.

Finally, eq 3 also allows us to broaden the interpretation of our data. Specifically, in theorizing Model 2, it was assumed that the doubly oxidized pair of P-clusters (i.e., P^{Ox}–P^{Ox}) became diamagnetic. Equation 3, however, suggests that this requirement is too restrictive. What is important is that the paramagnetism changes during the oxidation. In other words, in going from P^{Ox}–P to P^{Ox}–P^{Ox}, the magnetic interaction need only *decrease*; it does not have to go to zero. Therefore, P^{Ox}–P^{Ox} must have a J_P and/or T_{1P} which yields a reduction in $1/T_1T_2$ compared to that of P^{Ox}–P.

How much reduction is needed? Assume that P^{Ox}–P produces a magnetic interaction which increases $\Delta P_{1/2}$ by an amount α while the doubly oxidized clusters, P^{Ox}–P^{Ox}, increase it by $2\alpha/n$, where n is the reduction factor with $n > 1$. Figure 7 shows the theoretical variation in $\Delta P_{1/2}$ during oxidation for different values of n. In these plots, when $n = 1$, the P-clusters are independent and behave as predicted by Model 1 (i.e., all oxidized P-clusters impart the same magnetic effect). On the other hand, Model 2 (i.e., where P^{Ox}–P^{Ox} is diamagnetic) is equivalent to setting $n = \infty$. Therefore, as n increases from 1 to ∞, the relative values of $\Delta P_{1/2}$ will change from those observed for Model 1 to those for Model 2. Figure 7 shows the calculated variations in $\Delta P_{1/2}$ for different values of n and demonstrates that, within the experimental uncertainty of our data, it is only necessary that $n \geq 4$. This result is extremely important; it means that *both* P^{Ox}–P and P^{Ox}–P^{Ox} states can be paramagnetic so long as there is a change in J_P in going from P^{Ox}–P to P^{Ox}–P^{Ox} such that $n \geq 4$, as defined above.

The only data shown in Figure 6 not yet discussed are the increases in $\Delta P_{1/2}$ observed upon addition of the 5th oxidizing equiv. This is an unexpected result, since at this point all the P-clusters should be oxidized and the 5th equiv should only oxidize half the M-centers, causing them to become diamagnetic. The source of this increase is unknown, but its presence suggests that the effective paramagnetism of the P-clusters is somehow coupled to the state of oxidation of the M-centers. It is interesting to note that a similar trend has been shown to exist[28] in the magnetic susceptibility (χ) measurements of Av1 during oxidation, which show a similar increase (and not a decrease, as might be expected as the protein becomes less paramagnetic) in χ between the 4th and 5th oxidizing equiv.

In summary, magnetic interactions have been detected between paramagnetic P-clusters and M-centers which are probably dipolar in origin. The variation in the degree of these interactions during P-clusters' oxidation is interpreted in terms of the P-clusters existing as interactive pairs which are oxidized 1 equiv at a time and where both the singly and doubly oxidized state can be paramagnetic.

Acknowledgment. We gratefully acknowledge the financial support of the National Institutes of Health (Grant No. GM 33965).

Registry No. FeMoCo, 72994-52-6; nitrogenase, 9013-04-1.

(28) Smith, J. P.; Emptage, M. H.; Orme-Johnson, W. H. *J. Biol. Chem.* **1982**, *257*, 2310–2313.